Development 140, 1785-1795 (2013) doi:10.1242/dev.089763

Lis1 mediates planar polarity of auditory hair cells through regulation of microtubule organization

Conor W. Sipe, Lixia Liu*, Jianyi Lee, Cynthia Grimsley-Myers‡ and Xiaowei Lu§

SUMMARY

The V-shaped hair bundles atop auditory hair cells and their uniform orientation are manifestations of epithelial planar cell polarity (PCP) required for proper perception of sound. PCP is regulated at the tissue level by a conserved core Wnt/PCP pathway. However, the hair cell-intrinsic polarity machinery is poorly understood. Recent findings implicate hair cell microtubules in planar polarization of hair cells. To elucidate the microtubule-mediated polarity pathway, we analyzed Lis1 function in the auditory sensory epithelium in the mouse. We show that conditional deletion of *Lis1* in developing hair cells causes defects in cytoplasmic dynein and microtubule organization, resulting in planar polarity defects without overt effects on the core PCP pathway. *Lis1* ablation during embryonic development results in defects in hair bundle morphology and orientation, cellular organization and junctional nectin localization. We present evidence that Lis1 regulates localized Rac-PAK signaling in embryonic hair cells, probably through microtubule-associated Tiam1, a guanine nucleotide exchange factor for Rac. *Lis1* ablation in postnatal hair cells significantly disrupts centrosome anchoring and the normal V-shape of hair bundles, accompanied by defects in the pericentriolar matrix and microtubule organization. Lis1 is also required for proper positioning of the Golgi complex and mitochondria as well as for hair cell survival. Together, our results demonstrate that Lis1 mediates the planar polarity of hair cells through regulation of microtubule organization downstream of the tissue polarity pathway.

KEY WORDS: Lis1, Pafah1b1, PCP, Rac GTPase, Dynein, Microtubule, Stereociliary bundle, Nectin, Deafness

INTRODUCTION

In addition to apical-basal polarity, planar cell polarity (PCP), or polarity within an epithelial cell sheet, is crucial for epithelial morphogenesis and function. Sensory hair cells are specialized neuroepithelial cells that convert mechanical stimuli into electrical nerve impulses. Mechanotransduction is accomplished by the V-shaped stereociliary bundle (or hair bundle) located on the apex of each hair cell. Each hair bundle consists of rows of actin-based stereocilia arranged in a staircase pattern with a single microtubule-based kinocilium next to the tallest row of stereocilia. This polarized structure renders the hair bundle directionally sensitive to deflections (Kazmierczak and Müller, 2012). As a result, hair cells must be uniformly oriented across the plane of the auditory sensory epithelium, the organ of Corti, such that the vertex of each bundle points toward the lateral edge of the cochlear duct. Proper hair bundle polarity and orientation are essential for normal hearing.

Hair cell planar polarity is established during embryogenesis in vertebrates. One of the earliest manifestations of planar polarization is the migration of the axonemal kinocilium from the center of the hair cell apex toward the cell periphery (Denman-Johnson and Forge, 1999; Tilney et al., 1992). The kinocilium is a specialized primary cilium that extends from the basal body located just below the apical surface. Following its migration toward the lateral edge of the cochlear duct, microvilli adjacent to the kinocilium thicken and elongate, eventually forming a V-shaped bundle of stereocilia, with the kinocilium at its vertex. Nascent hair bundles then refine and align their orientation during late embryonic and early postnatal development (Dabdoub et al., 2003). Thus, positioning of the kinocilium/basal body near the lateral pole is tightly coupled with hair bundle polarity and orientation, and together they constitute morphological features of hair cell planar polarity.

Hair cell planar polarity is coordinated at the tissue level by an evolutionarily conserved core Wnt/PCP pathway (Goodrich and Strutt, 2011). Downstream of the core PCP genes, the small GTPase Rac and its effector p21-activated kinases (PAKs) have been shown to mediate basal body positioning and hair bundle orientation (Grimsley-Myers et al., 2009; Sipe and Lu, 2011). Wnt/PCP signaling spatially orients localized Rac-PAK signaling on the hair cell cortex (Grimsley-Myers et al., 2009); however, the underlying mechanisms remain incompletely understood.

Accumulating evidence suggests that tissue-level PCP signaling impinges on a hair cell-intrinsic pathway that controls the planar polarization of individual hair cells. The kinocilium and its connection to the adjacent stereocilium, via the kinociliary links, are required for the normal V-shape and orientation of the nascent hair bundle (Jones et al., 2008; Sipe and Lu, 2011; Webb et al., 2011). Moreover, a non-ciliary function of Kif3a, a component of the kinesin II plus-end-directed microtubule motor complex, coordinates basal body positioning and hair bundle orientation through spatial regulation of Rac-PAK signaling, thus implicating microtubule-based intracellular transport in hair cell planar polarization (Sipe and Lu, 2011). In addition to templating the kinocilium, the basal body (or the mother centriole), along with the daughter centriole and the associated pericentriolar matrix, organize cytoplasmic microtubules in hair cells (Steyger et al., 1989).

To further elucidate the microtubule-mediated hair cell polarity pathway, we investigated the function of a well-established microtubule regulator, Lis1 (Pafah1b1 – Mouse Genome

Department of Cell Biology, University of Virginia Health System, Charlottesville, VA 22908, USA.

*Present address: Department of Medicine, Allergy and Immunology, University of Virginia, Charlottesville, VA 22908, USA
‡Present address: Department of Cell Biology, Emory University School of Medicine, Atlanta, GA 30322, USA
§Author for correspondence (xl6f@virginia.edu)

Accepted 11 February 2013

Informatics). *LIS1* mutations cause type I lissencephaly, a human brain malformation (Wynshaw-Boris et al., 2010). Functionally, Lis1 controls microtubule organization as a microtubule-associated protein and regulator of cytoplasmic dynein, a minus-end-directed microtubule motor complex that participates in a range of cellular processes, including cell migration, organelle positioning and mitotic spindle assembly (Huang et al., 2012; Vallee and Tsai, 2006; Vallee et al., 2012). Lis1 regulates the localization of dynein to microtubule plus ends and the cell cortex, as well as the motor function of dynein (Huang et al., 2012; McKenney et al., 2010). In addition to mediating dynein function, Lis1 also regulates actin dynamics and Rho GTPase signaling (Kholmanskikh et al., 2003; Kholmanskikh et al., 2006; Rehberg et al., 2005). Thus, Lis1 is a strong candidate regulator of hair cell planar polarity.

Here, we analyzed the inner ears of conditional *Lis1* mouse mutants during embryonic and postnatal development. *Lis1* mutant embryos show defects in hair cell planar polarity and cellular organization of the organ of Corti due to impaired Rac-PAK signaling. We also uncover a crucial role for Lis1 in maintaining planar polarity in postnatal hair cells by regulating cytoplasmic dynein and microtubule organization. Lastly, our results reveal a function of Lis1-dynein in organelle positioning and hair cell survival.

MATERIALS AND METHODS

Mice

Animal care and use were in compliance with NIH guidelines and the Animal Care and Use Committee at the University of Virginia. Mice were obtained from the Jackson Laboratory or the referenced sources and maintained on a mixed genetic background. The morning of a plug was designated as embryonic day (E) 0.5 and the day of birth as postnatal day (P) 0. For embryonic experiments, $Atoh1^{Cre}$; $Lis1^{+/-}$ mice were mated with $Lis1^{flox/flox}$ mice to generate $Atoh1^{Cre}$; $Lis1^{flox/-}$ progeny (referred to as $Lis1^{cKO\text{-}early}$). Although $Lis1^{cKO\text{-}early}$ embryos were recovered in close to the expected Mendelian ratio until E18.5 (28/138=20.3%; expected: 25%), they rarely survived birth. For postnatal experiments, $Atoh1^{Cre}$; $Lis1^{flox/+}$ mice were crossed with $Lis1^{flox/flox}$ mice to generate $Atoh1^{Cre}$; $Lis1^{flox/flox}$ progeny with or without *GFP-centrin2* (referred to $Lis1^{cKO\text{-}late}$). $Lis1^{cKO\text{-}late}$ mice were born in the expected Mendelian ratio (86/382=22.5%; expected: 25%) and survived until postnatal stages. $Lis1^{flox/-}$ mice did not exhibit any inner ear phenotypes; nor did $Lis1^{flox/+}$ mice with or without $Atoh1^{Cre}$, which served as controls. The *GFP-centrin2* transgenic line (Higginbotham et al., 2004) was used to mark the centrioles. The following genotyping primers were used: 5′-AGAACCTGAAGATGTTCGCG-3′ and 5′-GGCTATAC-GTAACAGGGTGT-3′ for *Cre*; 5′-TGAATGCATCAGAACCATGC-3′ and 5′-CCTCTACCACTAAAGCTTGTTC-3′ for $Lis1^{flox}$ and $Lis1^{+}$; 5′-ATCTCCGATGTTTGAGTATG-3′ and 5′-CCTCTACCACTAAAGC-TTGTTC-3′ for $Lis1^{-}$.

Immunohistochemistry and image acquisition

Otic capsules were dissected from mice of the indicated ages and fixed in 4% paraformaldehyde for 1 hour at room temperature or overnight at 4°C. For dishevelled 2, dynein intermediate chain, Pcm1, Rac1-GTP, pan-Rac1 and mitochondrial immunostaining, otic capsules were fixed in 10% trichloroacetic acid for 1 hour on ice. Cochleae were dissected from otic capsules, and immunohistochemistry was carried out as previously described (Grimsley-Myers et al., 2009). For cryosectioning, paraformaldehyde-fixed otic capsules were dissected, embedded and snap frozen in OCT (Tissue-Tek) and then cryosectioned at 14 μm.

The following primary antibodies were used for immunostaining: Lis1 (1:50, Santa Cruz Biotechnology; or 1:250, Abcam), dishevelled 2 (1:100), phospho-ERM (ezrin/radixin/moesin) (1:1000) and cleaved caspase 3 (1:200) (Cell Signaling), Rac1 (1:100; Millipore), Rac1-GTP (1:500; NewEast Biosciences), myosin VI (1:1000) and myosin VIIa (1:1000) (Proteus Biosciences), E-cadherin (1:200), α-tubulin (1:1000), β1/β2-tubulin and acetylated tubulin (1:500) (Sigma), $p27^{kip1}$ (Cdkn1b – Mouse Genome Informatics) (1:200; Thermo Scientific), nectin-1 and nectin-3 (1:100; MBL), nectin-2 (1:200; Epitomics), Tiam1 (1:100; Santa Cruz Biotechnology), dynein intermediate chain (74.1, 1:100; gift from Dr Kevin Pfister, University of Virginia), Pcm1 (1:400; gift from Dr Andreas Merdes, CNRS/Université de Toulouse), GM130 (Golga2 – Mouse Genome Informatics) (1:250; BD Biosciences) and anti-mitochondria (1:50; Abcam). Alexa Fluor-conjugated secondary antibodies (1:1000), Alexa Fluor 488- and Rhodamine-conjugated phalloidin (1:200), and Hoechst 33342 (1:10,000) were obtained from Invitrogen.

z-stacks of images were collected using a Deltavision deconvolution microscope equipped with a 60× objective (NA 1.4) using the Softworx package (Applied Precision). Alternatively, image stacks were collected using a Zeiss LSM 510 confocal microscope equipped with a 100× objective (NA 1.4) using Zeiss image acquisition software. Optical slices and maximum intensity projections were generated using the Zeiss LSM Image Browser program or ImageJ 1.45s (NIH). All images shown were taken from the mid-basal region of the cochlea (25% length) unless otherwise indicated.

Scanning electron microscopy was carried out as described previously (Sipe and Lu, 2011).

Western blotting

Because the indicated lot of anti-phospho-Pak1/2/3 antibody failed to detect specific signals by immunostaining, we instead used it to quantify the relative levels of phospho-PAK (pPAK) by immunoblotting. Immunoblots were carried out as described previously (Lee et al., 2012). Primary antibodies were: anti-Pak1 (Cell Signaling), anti-phospho-Pak1/2/3 (Invitrogen #44940G, lot #980627A) and anti-Gapdh (Ambion). The levels of Pak1 and pPAK were normalized to their respective Gapdh loading controls, and the ratio of normalized levels of pPAK to Pak1 in each sample was calculated. Data from control (n=9) and $Lis1^{cKO\text{-}early}$ (n=5) samples were tested for significance using Student's t-test and data are presented as mean ± s.e.m.

Quantification of hair cell phenotypes

Quantification of hair bundle orientation was carried out as described previously (Sipe and Lu, 2011). Data in the text are presented as mean ± s.e.m. To quantify the distance of the centrosome from the cell membrane, the distance along a line drawn from the center of the centrosome to the closest edge of the cell was measured using ImageJ. For all experiments, measurements were obtained from hair cells in the basal region of the cochlea (15% cochlear length; at least three cochleae per genotype).

RESULTS

Lis1 is localized to the pericentriolar region in developing hair cells

To investigate a potential role for Lis1 in auditory hair cell development, we first determined the subcellular localization of Lis1 in the developing organ of Corti. At E17.5, Lis1 was detected on the stereocilia and the hair cell centrioles (Fig. 1A-C). At P1, Lis1 was prominently localized to the pericentriolar region in hair cells, forming a cloud surrounding the centrioles, and was also detected at low levels on the centrioles of supporting cells (Fig. 1D-F). These localization patterns are consistent with those reported in other cell types and suggest a function for Lis1 in the regulation of the hair cell microtubule network (Sasaki et al., 2000; Tanaka et al., 2004).

Lis1 deletion during embryonic development causes defects in hair bundle morphology and orientation

To investigate the function of Lis1 in developing hair cells, we generated conditional mutants using a floxed allele of *Lis1* (Hirotsune et al., 1998) and an $Atoh1^{Cre}$ driver line that expresses Cre in developing hair cells and a subset of supporting cells starting at ~E14.5 (Yang et al., 2010). We also used a null allele (Lis^{-}) derived from the $Lis1^{flox}$ allele by germline Cre expression. To perturb Lis1 function in embryonic hair cells, we generated $Atoh1^{Cre}$; $Lis1^{flox/-}$ embryos (hereafter referred to as $Lis1^{cKO\text{-}early}$).

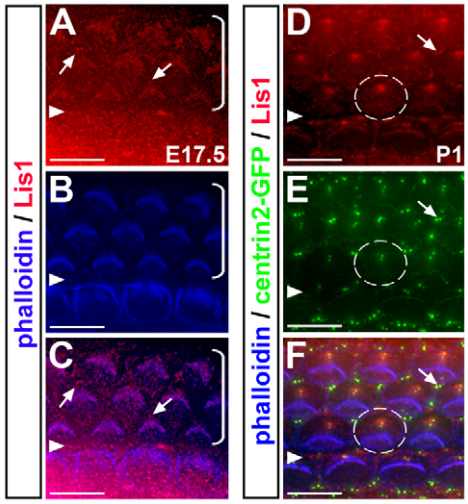

Fig. 1. Lis1 expression in developing hair cells. Immunostaining for Lis1 (red) and phalloidin staining (blue) in flat-mounted cochleae. (**A-C**) At E17.5, Lis1 is localized along the stereocilia and on the centrioles (arrows). (**D-F**) At P1, Lis1 is found in a diffuse cloud around hair cell centrioles and on the centrioles of supporting cells (arrows). Centrioles are marked with GFP-centrin2 (green). White circles outline hair cell boundaries. Arrowheads mark the pillar cell row and brackets indicate outer hair cell rows. Scale bars: 6 µm.

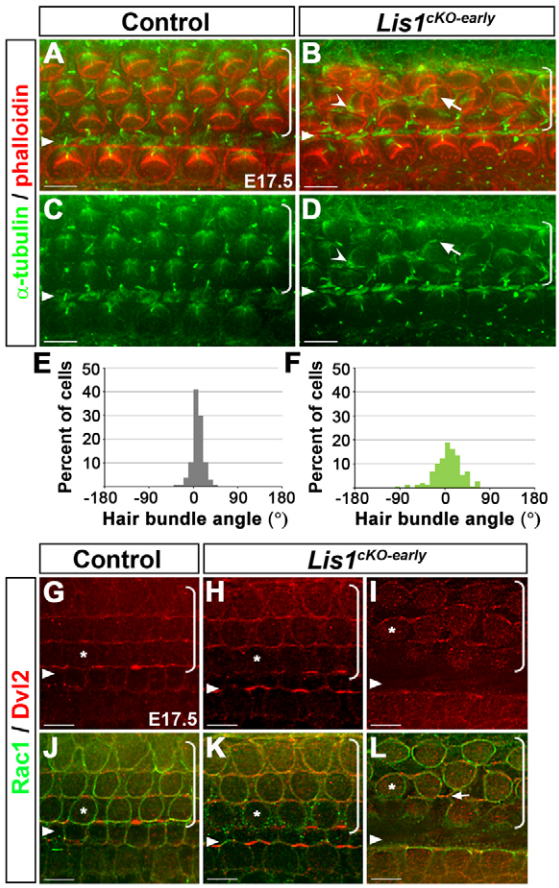

Fig. 2. Planar polarity and microtubule defects in the *Lis1*$^{cKO\text{-}early}$ organ of Corti. (**A-D**) E17.5 control (A,C) and *Lis1*$^{cKO\text{-}early}$ (B,D) cochleae stained with phalloidin (red) and for α-tubulin (green) to label the hair bundle and microtubules, respectively. Arrows indicate a flattened hair bundle with an off-center kinocilium. Arrowheads indicate a mispositioned centrosome. (**E**,**F**) Quantification of hair bundle orientation in E18.5 control (E; *n*=137) and *Lis1*$^{cKO\text{-}early}$ (F; *n*=148) cochleae. (**G-L**) Dvl2 immunostaining (red) in control (G,J) and *Lis1*$^{cKO\text{-}early}$ (H,K and I,L show two representative images) organ of Corti. Asterisks indicate examples of hair cells with Dvl2 staining on the lateral pole. Arrow in L indicates Dvl2 staining on the cell contact between two supporting cells. Cell boundaries are labeled by Rac1 immunostaining (green). Triangular arrowheads mark the pillar cell row and brackets indicate outer hair cell rows. Scale bars: 6 µm.

At E17.5, a subset of *Lis1*$^{cKO\text{-}early}$ hair cells had bundles with an abnormal, flattened morphology (Fig. 2B). Moreover, *Lis1*$^{cKO\text{-}early}$ hair cells displayed hair bundle misorientation (Fig. 2B,F; average bundle deviation of 20.1±1.5°) compared with littermate controls (Fig. 2A,E; average bundle deviation of 8.6±0.7°). We also examined the position of the kinocilium and found that it had migrated to the hair cell periphery (Fig. 2B). However, kinocilia were often mispositioned with respect to both the hair bundle and the medial-lateral axis of the cochlea (Fig. 2B,D). These defects in kinocilium/basal body positioning correlated with hair bundle misorientation. Furthermore, in contrast to the regular aster-shaped array in control hair cells (Fig. 2C), cytoplasmic microtubules appeared disorganized in *Lis1*$^{cKO\text{-}early}$ hair cells (Fig. 2D). These results demonstrate that Lis1 regulates the microtubule organization and planar polarization of embryonic hair cells.

Hair bundle orientation is coordinated by the core Wnt/PCP pathway (Goodrich and Strutt, 2011). Therefore, we sought to determine whether Wnt/PCP signaling is compromised in *Lis1*$^{cKO\text{-}early}$ cochleae by examining the asymmetric membrane localization of the core PCP protein dishevelled 2 (Dvl2). In E17.5 wild-type cochleae, Dvl2 was localized to the lateral side of hair cell membranes (Fig. 2G,J). This localization was essentially unchanged in *Lis1*$^{cKO\text{-}early}$ hair cells (Fig. 2H,I,K,L). Of note, the hair cell rows in *Lis1*$^{cKO\text{-}early}$ cochleae were slightly jumbled, and abnormal apical contacts between two supporting cells with Dvl2 staining were observed (Fig. 2L). These results demonstrate that Lis1 is not required for the asymmetric membrane localization of Dvl2, suggesting that Wnt/PCP signaling is at least partially active in *Lis1*$^{cKO\text{-}early}$ hair cells.

Defective cellular organization and nectin localization in *Lis1*$^{cKO\text{-}early}$ organ of Corti

To further assess cellular organization in *Lis1*$^{cKO\text{-}early}$ cochleae, we stained E18.5 tissue for myosin VI and β1/β2-tubulin to label hair cells and supporting cells, respectively. Instead of the normal 'checkerboard' pattern of hair cells interdigitated with supporting cells (Fig. 3A), pairs of *Lis1*$^{cKO\text{-}early}$ hair cells often appeared to be in direct contact, without an intervening supporting cell (Fig. 3B). Moreover, the apical surfaces of both hair cells and supporting cells in *Lis1*$^{cKO\text{-}early}$ cochleae were misshapen. Many hair cells adopted an oblong or irregular shape and the evenly spaced 'hourglass' shape of supporting cell apical domains was frequently jumbled and distorted (Fig. 3B). We next examined transverse cochlear sections. In control sections, hair cell nuclei were invariably located a uniform distance from the luminal surface of the epithelium (Fig. 3C). By contrast, the *Lis1*$^{cKO\text{-}early}$ sensory epithelium was disorganized, with hair cell nuclei frequently found at varying distances from the luminal surface (Fig. 3D).

The checkerboard pattern of the organ of Corti is regulated by the nectin (or poliovirus receptor-related) family of cell adhesion molecules (Togashi et al., 2011). We examined the localization of

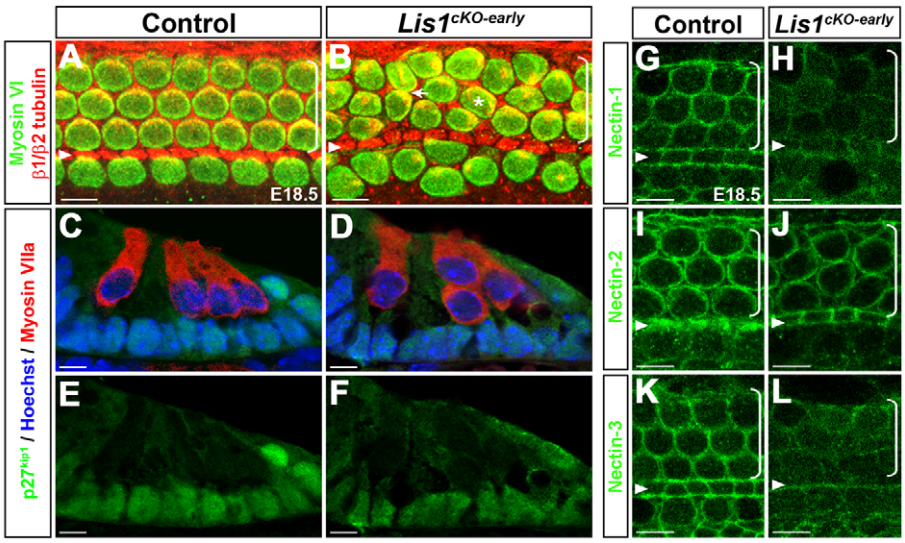

Fig. 3. Lis1 regulates cellular organization and junctional nectin localization in the organ of Corti. (**A**,**B**) Myosin VI (green) and β1/β2-tubulin (red) immunostaining in E18.5 control (A) and *Lis1*$^{cKO\text{-}early}$ (B) cochleae. The arrow in B indicates two hair cells in contact with one another and the asterisk marks a hair cell of an abnormal shape. (**C-F**) Transverse sections of E18.5 control (C,E) and *Lis1*$^{cKO\text{-}early}$ (D,F) cochleae stained for the supporting cell marker p27^{kip1} (green), the hair cell marker myosin VIIa (red) and with Hoechst (blue) to label cell nuclei. (**G-L**) Localization of nectin-1 (G,H), nectin-2 (I,J) and nectin-3 (K,L) in E18.5 control (G,I,K) and *Lis1*$^{cKO\text{-}early}$ (H,J,L) organ of Corti. Arrowheads mark the pillar cell row and brackets indicate outer hair cell rows. Scale bars: 6 μm.

nectin-1, -2 and -3 in E18.5 cochleae. In the control, all three nectins were localized to hair cell-supporting cell contacts, consistent with their role in mediating heterotypic adhesion between these two cell types (Togashi et al., 2011) (Fig. 3G,I,K). By contrast, localization of all three nectins at cell-cell contacts was reduced in *Lis1*$^{cKO\text{-}early}$ cochleae, with nectin-1 and -3 being more affected than nectin-2 (Fig. 3H,J,L). By contrast, the junctional localization of E-cadherin was not significantly changed (supplementary material Fig. S1). These results suggest that impaired nectin-mediated cell adhesion contributes to the cellular organization defects in the *Lis1*$^{cKO\text{-}early}$ organ of Corti.

Lis1 regulates Rac-PAK signaling in embryonic hair cells

Given the role of Lis1 as a regulator of cytoplasmic dynein in other systems, we investigated dynein localization using an antibody against the dynein intermediate chain (Dillman et al., 1994). Immunostaining of E17.5 control hair cells revealed a cloud of dynein in the apical cytoplasm, with a higher concentration in the pericentriolar region (supplementary material Fig. S2A). In *Lis1*$^{cKO\text{-}early}$ hair cells, dynein was still found in the pericentriolar region, but it was more diffuse (supplementary material Fig. S2A), indicating a role of Lis1 in regulating dynein localization in hair cells.

To further determine the mechanisms underlying the planar polarity and cellular organization defects, we next examined Rac-PAK signaling in *Lis1*$^{cKO\text{-}early}$ cochleae. Our previous work suggests a model in which microtubule-mediated transport regulates the localized activation of Rac-PAK signaling on the hair cell cortex (Sipe and Lu, 2011). This model predicts that regulators of microtubule organization may be important for cortical Rac-PAK signaling. In support of this idea, *Lis1*$^{cKO\text{-}early}$ and *Rac1*^{cKO} mutants have similar planar polarity and cellular organization defects (Grimsley-Myers et al., 2009). To further test this hypothesis, we measured the levels of activated PAK using a pPAK antibody. Immunoblotting of *Lis1*$^{cKO\text{-}early}$ cochleae showed a significant decrease (P=0.006) in the ratio of pPAK to total Pak1 in mutants (0.77±0.05) compared with controls (1.14±0.09) (Fig. 4A).

To more directly assess Rac signaling *in situ*, we examined the localization of active GTP-bound Rac1 in E17.5 cochleae using an antibody specific for Rac1-GTP alongside a pan-Rac1 antibody to localize simultaneously the total pool of Rac1. In agreement with previously reported pPAK localization (Grimsley-Myers et al., 2009; Sipe and Lu, 2011), Rac1-GTP was enriched on the lateral hair cell cortex in the control, whereas total Rac1 was uniformly distributed along the circumference of the hair cell (Fig. 4B,D,F,H). Rac1-GTP was also detected in the pericentriolar region and on the stereocilia (supplementary material Fig. S2B). In *Lis1*$^{cKO\text{-}early}$ cochleae, the cortical domain of Rac1-GTP was significantly reduced and/or misoriented relative to the medial-lateral axis of the cochlea (Fig. 4C,E,G,I). Localization of Rac1-GTP in the pericentriolar region was also disorganized and diffuse, although it was still detected on the hair bundle (supplementary material Fig. S2B). These results indicate that Lis1 regulates localized Rac1 activity at the hair cell cortex and other subcellular locations.

Rac GTPases are activated by guanine nucleotide exchange factors (GEFs) and inactivated by GTPase-activating proteins (GAPs). To investigate the molecular mechanisms of Lis1- and microtubule-mediated Rac activation, we searched the literature for Rac GEFs with reported localization to microtubules in other cell types. T-cell lymphoma invasion and metastasis 1 (Tiam1) emerged as the leading candidate. Tiam1 associates with microtubules in neurons and regulates neuronal polarity (Kunda et al., 2001). Furthermore, the Tiam1 homolog Tiam2 (or STEF) has been shown to mediate microtubule-dependent Rac activation during cell migration (Rooney et al., 2010). Importantly, cochlear explants treated with NSC23766, a competitive inhibitor of Rac interactions with certain GEFs, including Tiam1 (Akbar et al., 2006), showed planar polarity defects (Sipe and Lu, 2011). At E17.5, Tiam1 is highly enriched on microtubules and the kinocilium in control hair cells (Fig. 4J,L,N; supplementary material Fig. S2C-E). In *Lis1*$^{cKO\text{-}early}$ hair cells, although still detected on microtubules, Tiam1 staining was greatly disorganized or diminished in cells with disorganized microtubules (Fig. 4K,M,O). These data suggest a potential role for microtubule-associated Tiam1 in stimulating cortical Rac-PAK activity.

Lis1 is required to maintain the V-shape of hair bundles during postnatal development

Having demonstrated a role for Lis1 in planar polarization in embryonic hair cells, we next sought to determine the function of Lis1 in postnatal hair cells. We generated *Atoh1*^{Cre}; *Lis1*$^{flox/flox}$ mice (hereafter referred to *Lis1*$^{cKO\text{-}late}$). In contrast to *Lis1*$^{cKO\text{-}early}$

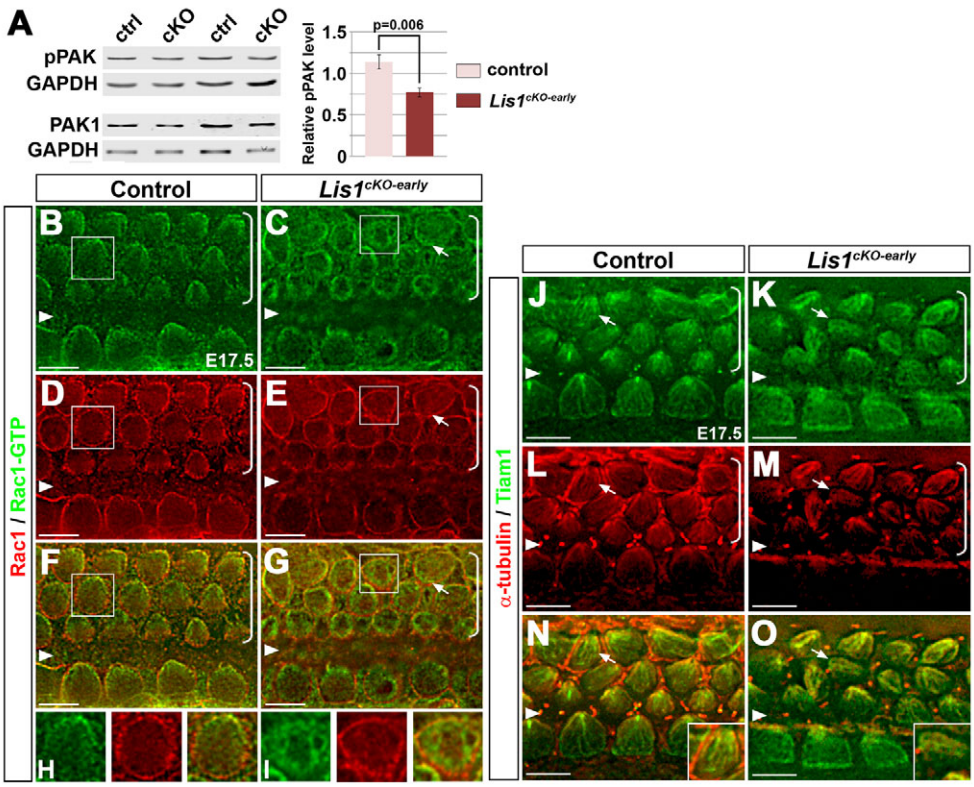

Fig. 4. Lis1 mediates cortical Rac-PAK signaling, probably through microtubule-associated Tiam1. (**A**) Western blot analysis of the levels of pPAK and Pak1 in control (ctrl) and *Lis1*$^{cKO\text{-}early}$ (cKO) cochleae. Lysates of two cochleae from the same embryo were pooled and loaded in each lane. Gapdh served as loading control. Error bars indicate s.e.m. (**B-I**) Localization of Rac1-GTP (green) and total Rac1 (red) in E17.5 control (B,D,F,H) and *Lis1*$^{cKO\text{-}early}$ (C,E,G,I) cochleae. Boxed control and *Lis1*$^{cKO\text{-}early}$ cells are shown at higher magnification in H and I, respectively. (**J-O**) Colocalization of Tiam1 (green) and α-tubulin (red) in E17.5 control (J,L,N) and *Lis1*$^{cKO\text{-}early}$ (K,M,O) organ of Corti. The cells indicated by arrows are shown at higher magnification in the insets. Arrowheads mark the pillar cell row and brackets indicate outer hair cell rows. Scale bars: 6 μm.

mutants, two Cre-mediated recombination events are required to generate a *Lis1*-deficient hair cell. Since Lis1 protein levels correlate tightly with gene dosage (Gambello et al., 2003), we reasoned that the combined effects of slower DNA excision and longer protein perdurance in *Lis1*$^{cKO\text{-}late}$ would enable slower depletion of Lis1 compared with *Lis1*$^{cKO\text{-}early}$ mutants.

At P0, the *Lis1*$^{cKO\text{-}late}$ organ of Corti exhibited normal cellular organization (Fig. 5B). Hair bundle morphology and orientation were also normal, suggesting that Lis1 function in the *Lis1*$^{cKO\text{-}late}$ cochlea was sufficient to sustain the embryonic phase of hair cell morphogenesis. However, starting at ~P2 and following a base-to-apex gradient along the cochlea, some *Lis1*$^{cKO\text{-}late}$ outer hair cells displayed hair bundle morphology defects ranging from a flattened bundle (Fig. 5D,F,G) to splitting of the bundle into two separate groups of stereocilia (Fig. 5D,H-J). Rarely, hair bundles were severely dysmorphic or completely fragmented (Fig. 5K). Overall, 13% of *Lis1*$^{cKO\text{-}late}$ hair bundles in outer hair cell rows exhibited a flattened morphology, 8% were split, and 1% were dysmorphic (Fig. 5E). By contrast, *Lis1*$^{cKO\text{-}late}$ vestibular hair cells in the utricular macula at P4 had no overt defects in hair bundle morphology or orientation (supplementary material Fig. S3). These results indicate that, in addition to its earlier function, Lis1 is required for maintaining the normal V-shape of the auditory hair bundle during postnatal development.

Lis1 mediates the positioning of the hair cell centrosome near the lateral cortex

To understand the basis for the hair bundle defects in *Lis1*$^{cKO\text{-}late}$ hair cells, we examined basal body positioning at P2. In control hair cells, the centrosome (the basal body and daughter centriole) was invariably found near the lateral pole and aligned along the medial-lateral axis of the cochlear duct (Fig. 5L). By contrast, the centrosome in many *Lis1*$^{cKO\text{-}late}$ hair cells was located away from the lateral pole and toward the center of the cell, particularly in those cells with a flattened or split hair bundle (Fig. 5M). Indeed, the distance between the centrosome and the lateral hair cell membrane ($D_{C\text{-}M}$) closely correlated with hair bundle morphology defects (Fig. 5N). On average, $D_{C\text{-}M}$ in *Lis1*$^{cKO\text{-}late}$ hair cells with a normal bundle morphology (0.90±0.05 μm; n=42) was similar to that of controls (0.87±0.02 μm; n=60). However, $D_{C\text{-}M}$ was dramatically increased in *Lis1*$^{cKO\text{-}late}$ hair cells with a flattened hair bundle (1.55±0.06 μm; n=45) and increased still further in cells with a split hair bundle (2.04±0.07 μm; n=34) (Fig. 5N). Thus, using basal body position and the V-shaped hair bundle as morphological readouts for planar polarity, we conclude that Lis1 is required for the maintenance of planar polarity in postnatal hair cells.

To investigate whether Wnt/PCP signaling plays a role in postnatal hair cells, we examined Dvl2 localization at P2. As in embryonic hair cells, Dvl2 was asymmetrically localized on the lateral hair cell membranes, suggesting a potential role for Wnt/PCP signaling in maintaining planar polarity (Fig. 6A,E). In *Lis1*$^{cKO\text{-}late}$ cochleae, asymmetric Dvl2 localization was unchanged (Fig. 6B,F), suggesting that Wnt/PCP signaling remains intact in *Lis1*$^{cKO\text{-}late}$ hair cells.

We also examined whether localized cortical Rac signaling persists in postnatal hair cells to maintain planar polarity. In control hair cells at P3, the cortical domain of Rac1-GTP on the lateral side of hair cells was no longer detectable (supplementary material Fig. S4A-C), whereas Rac1-GTP was still localized to the hair bundle and pericentriolar region (supplementary material Fig. S4D-I). Furthermore, Tiam1 localization to microtubules but not the kinocilium was greatly reduced compared with embryonic hair cells (supplementary material Fig. S4J-O). Together, these results suggest a developmental downregulation of Tiam1-mediated cortical Rac activation.

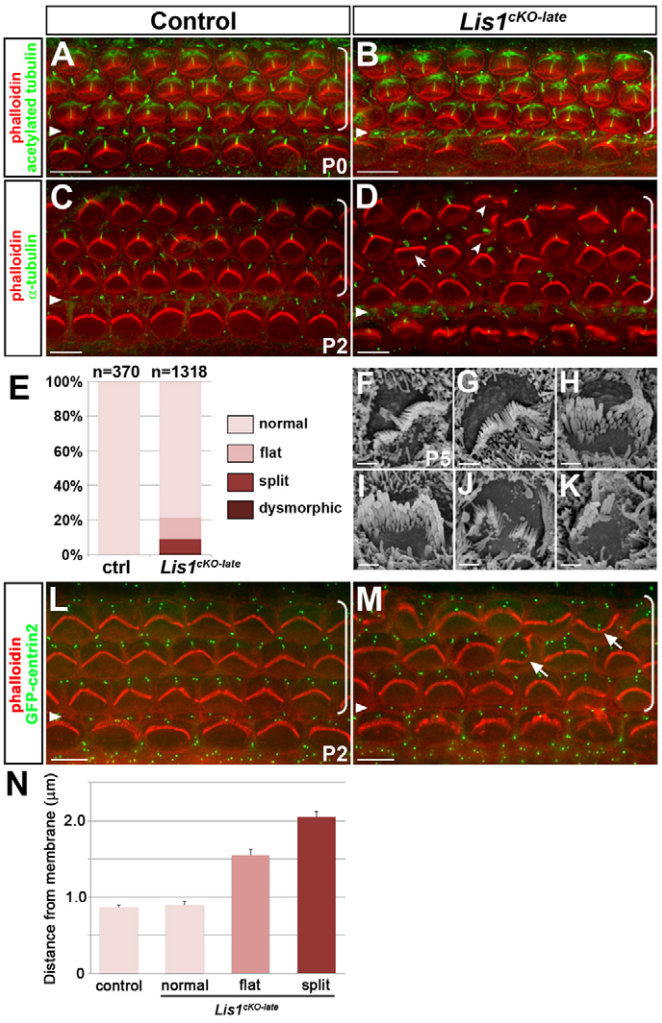

Fig. 5. Lis1 is crucial for maintaining hair bundle morphology and centrosome position in the postnatal organ of Corti. (**A**,**B**) Acetylated tubulin (green) and phalloidin (red) staining of P0 control (A) and *Lis1*$^{cKO\text{-}late}$ (B) cochleae. (**C**,**D**) α-tubulin (green) and phalloidin (red) staining of P2 control (C) and *Lis1*$^{cKO\text{-}late}$ (D) cochleae. (**E**) Penetrance of the hair bundle morphology phenotypes observed in *Lis1*$^{cKO\text{-}late}$ cochleae. (**F-K**) Scanning electron micrographs of P5 *Lis1*$^{cKO\text{-}late}$ outer hair cells showing hair cells with flattened (F,G), split (H-J) and dysmorphic (K) hair bundles. (**L**,**M**) Centrosome position (marked by GFP-centrin2, green) correlates with hair bundle morphology in P2 control (L) and *Lis1*$^{cKO\text{-}late}$ (M) hair cells. Arrows in M indicate *Lis1*$^{cKO\text{-}late}$ hair cells with split hair bundles and centrally placed centrosomes. (**N**) Quantification of the distance between the centrosome and the lateral hair cell membrane ($D_{C\text{-}M}$) in control and *Lis1*$^{cKO\text{-}late}$ hair cells. Error bars indicate s.e.m. Arrowheads mark the pillar cell row and brackets indicate outer hair cell rows. Scale bars: 6 μm in A-D,L,M; 2 μm in F-K.

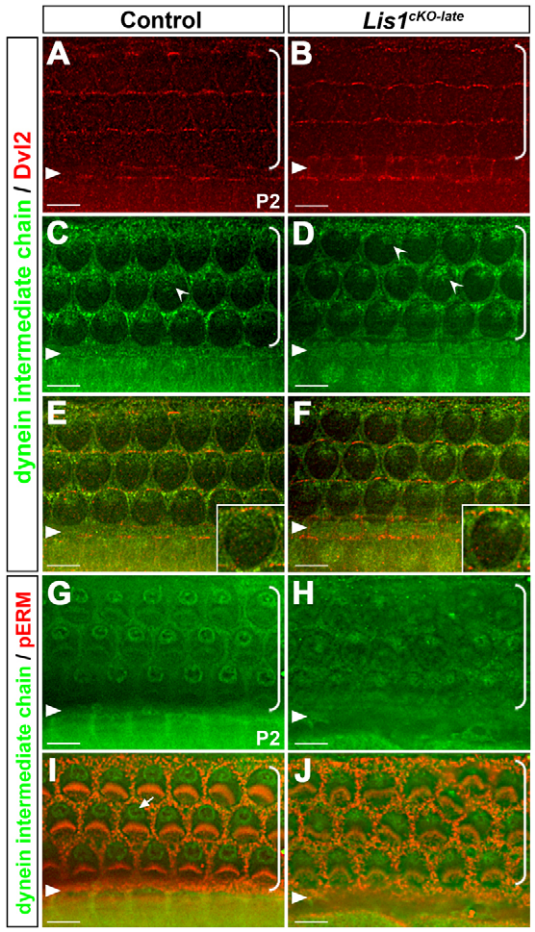

Fig. 6. Lis1 is required for dynein localization around the hair cell centrosome. (**A-F**) Immunostaining of Dvl2 (red) and dynein intermediate chain (green) in P2 control (A,C,E) and *Lis1*$^{cKO\text{-}late}$ (B,D,F) hair cells. Higher magnification insets in E and F show overlapping cortical staining of Dvl2 and dynein. Arrowheads indicate the basal terminus of the dynein lattice that surrounds the centrosome, which was more variable and irregular in shape in *Lis1*$^{cKO\text{-}late}$ hair cells (D). (**G-J**) Immunostaining of dynein intermediate chain (green) at the level of the hair cell centrosome in P2 control (G,I) and *Lis1*$^{cKO\text{-}late}$ (H,J) organ of Corti. Phospho-ERM (pERM, red) labels stereocilia and supporting cell microvilli. Triangular arrowheads mark the pillar cell row and brackets indicate outer hair cell rows. Scale bars: 6 μm.

Lis1 is required for proper dynein localization and pericentriolar matrix organization

To understand the basis for the centrosome positioning defects in *Lis1*$^{cKO\text{-}late}$ hair cells, we next examined the localization of cytoplasmic dynein. Immunostaining of dynein intermediate chain in control hair cells at P2 revealed a three-dimensional lattice of dynein in the pericentriolar region, extending from the centrosome basally for ~2 μm to the level of Dvl2 membrane localization (Fig. 6C). At the plane of the centrosome, dynein formed an organized ring surrounding the centrosome and also localized to one of the centrioles (Fig. 6G,I). Dynein staining was also detected on the cell cortex, partially overlapping with Dvl2 (Fig. 6E, inset). In *Lis1*$^{cKO\text{-}late}$ hair cells, instead of an organized three-dimensional lattice, dynein formed an irregular, diffuse cloud. At the plane of the centrosome, dynein collapsed inward toward the centrosome and was no longer detectable on centrioles (Fig. 6H,J). At the level of Dvl2 crescents, dynein was still detected extending basally from the pericentriolar cloud (Fig. 6D) and on the cell cortex, partially overlapping with Dvl2 (Fig. 6F, inset). These results indicate that Lis1 is required for normal dynein localization around the centrosome in hair cells.

Next we asked whether Lis1-dynein function is important for hair cell pericentriolar matrix organization, as in other cell types (Guo et al., 2006; Kubo et al., 1999; Zimmerman and Doxsey, 2000). We examined the localization of the pericentriolar material 1 (Pcm1) protein, a pericentriolar matrix component that is important for the

recruitment of other centrosomal proteins (Balczon et al., 1994; Dammermann and Merdes, 2002). In control hair cells at P3, Pcm1 was localized in a tight ring in the pericentriolar region, which formed interior to the dynein lattice ~0.2 µm below the daughter centriole (Fig. 7A,C, inset). By contrast, Pcm1 in *Lis1*$^{cKO\text{-}late}$ hair cells failed to organize into a ring-like structure and instead collapsed inward toward the centrioles, forming a diffuse cloud interior to the dynein clusters (Fig. 7B,D, inset). Thus, centrosome mispositioning in *Lis1*$^{cKO\text{-}late}$ hair cells is associated with dynein and pericentriolar matrix organization defects.

Microtubule organization defects in *Lis1*$^{cKO\text{-}late}$ hair cells

Lis1-dynein function in pericentriolar matrix organization regulates the interphase microtubule array in other systems (Quintyne et al., 1999; Smith et al., 2000). We therefore examined microtubule organization in *Lis1*$^{cKO\text{-}late}$ hair cells at P2, when hair bundle and dynein defects are beginning to manifest. In control hair cells, an aster-shaped radial microtubule array emanated from the pericentriolar matrix toward the cortex in all directions but was more prominent on the lateral side of the cell (Fig. 7E,G,I). Individual microtubules appeared to extend laterally and basally to contact the cortex and then curl around the circumference of the cell (Fig. 7I). In *Lis1*$^{cKO\text{-}late}$ hair cells, the organization of the cytoplasmic microtubule array was severely disrupted; the ring-like organization of the minus ends of microtubules collapsed inward and became more focused around the centrosome (Fig. 7F,H). This was particularly evident in *Lis1*$^{cKO\text{-}late}$ cells with flattened or split bundles (Fig. 7F,H,J, plane z). Instead of fanning out basally to form an aster-shaped array, microtubules in many *Lis1*$^{cKO\text{-}late}$ cells lacked apparent organization and directionality (Fig. 7F,H,J,K). In some cells, microtubules organized into thick bundles that wrapped around the circumference of the cell (Fig. 7J, plane z′). Overall, *Lis1*$^{cKO\text{-}late}$ hair cells appeared to have a reduced concentration of microtubules on the lateral side of the hair cell and more microtubules on the medial side of the cell (Fig. 7K, plane z′). Together, these results suggest that dynein and pericentriolar matrix defects in *Lis1*$^{cKO\text{-}late}$ hair cells result in disorganization of the microtubule network.

Lis1 deficiency leads to organelle distribution defects and subsequent outer hair cell death

In cultured cells, Lis1 and dynein regulate organelle position (Harada et al., 1998; Lam et al., 2010). We therefore determined whether the distributions of the Golgi and mitochondria were perturbed in *Lis1*$^{cKO\text{-}late}$ hair cells. At P2, the Golgi complex in control hair cells consisted of complex tubule structures (Fig. 8A) that were confined to a region just basal to the cuticular plate of the hair cell (Fig. 8B). Similarly, mitochondria were distributed throughout the cell body but were enriched in the apical cytoplasm (Fig. 8E,F). By contrast, in *Lis1*$^{cKO\text{-}late}$ hair cells, the Golgi complex appeared fragmented with vesicles spread throughout the cytoplasm (Fig. 8C,D). Mitochondria were also highly dispersed, and the apical population of mitochondria was greatly diminished (Fig. 8G,H). Taken together, these Golgi and mitochondria defects support a universal function of Lis1-dynein in organelle positioning.

To determine the fate of *Lis1*$^{cKO\text{-}late}$ hair cells, we examined *Lis1*$^{cKO\text{-}late}$ cochleae a few days after the onset of hair bundle and organelle defects. Beginning at ~P5 and proceeding in a wave from the basal region of the cochlea toward the apex, outer hair cells began to undergo apoptotic cell death, as indicated by cleaved caspase 3 immunostaining, and were extruded from the sensory epithelium (Fig. 8J). By P7, the basal region of the *Lis1*$^{cKO\text{-}late}$ cochlea was devoid of outer hair cells (Fig. 8M,N). These results reveal a requirement for Lis1 for auditory hair cell survival.

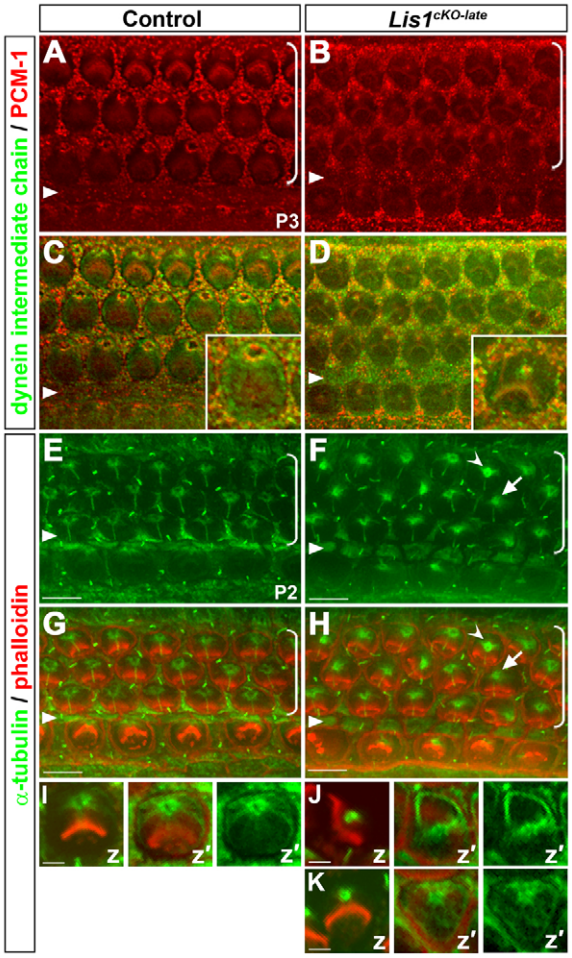

Fig. 7. Pericentriolar matrix and microtubule organization defects in *Lis1*$^{cKO\text{-}late}$ hair cells. (**A-D**) Immunostaining of Pcm1 (red) and dynein intermediate chain (green) in P3 control (A,C) and *Lis1*$^{cKO\text{-}late}$ (B,D) cochleae. Higher magnification insets in C and D show the distribution of Pcm1 in relation to dynein. (**E-K**) α-tubulin (green) and phalloidin (red) staining in P2 control (E,G,I) and *Lis1*$^{cKO\text{-}late}$ (F,H,J,K) cochleae. Arrows indicate a disorganized microtubule array. Arrowheads indicate inwardly collapsed microtubule minus ends. (I-K) Higher magnification optical sections of individual hair cells taken at the level of the hair cell basal body (z) and 1 µm basal to z (z′). Triangular arrowheads mark the pillar cell row and brackets indicate outer hair cell rows. Scale bars: 6 µm in A-H; 2 µm in I-K.

DISCUSSION

In this study, we have undertaken a comprehensive analysis of Lis1 and dynein function in developing auditory hair cells. Our results reveal a crucial function of Lis1 in dynein localization and microtubule organization and provide novel insights into the Lis1- and microtubule-mediated processes essential for hair cell planar polarity during both embryonic and postnatal development. In addition, we demonstrate that Lis1 is also required for proper organelle positioning and hair cell survival.

Together with recent advances, our results provide strong support for a two-tier hierarchy of hair cell planar polarity regulation. The core PCP pathway generates extrinsic or tissue polarity cues that

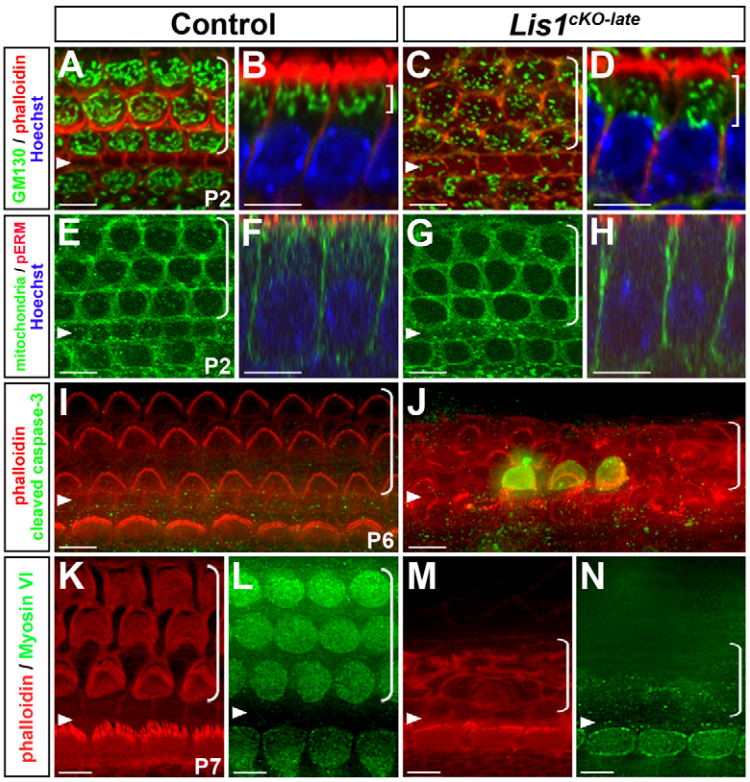

Fig. 8. Lis1 is required for organelle positioning and hair cell survival. (**A-D**) P2 control (A,B) and *Lis1*$^{cKO\text{-}late}$ (C,D) cochleae stained for the Golgi marker GM130 (green) and with phalloidin (red) and Hoechst (blue) to label cell nuclei. (B,D) Optical slices along the *z*-axis to show hair cells in profile, with brackets indicating the distribution of Golgi complexes in the apical cytoplasm. (**E-H**) P2 control (E,F) and *Lis1*$^{cKO\text{-}late}$ (G,H) organ of Corti stained for mitochondria (green), pERM (red) and with Hoechst (blue) to label cell nuclei. (F,H) Optical slices along the *z*-axis. (**I,J**) Cleaved caspase 3 (green) and phalloidin staining (red) in P6 control (I) and *Lis1*$^{cKO\text{-}late}$ (J) hair cells. *Lis1*$^{cKO\text{-}late}$ hair cells undergo apoptosis and are subsequently extruded from the epithelium. (**K-N**) Myosin VI (green) and phalloidin (red) staining in the basal region of P7 control (K,L) and *Lis1*$^{cKO\text{-}late}$ (M,N) cochleae. The *Lis1*$^{cKO\text{-}late}$ cochlea is devoid of outer hair cells. Arrowheads mark the pillar cell row and brackets (except B,D) indicate outer hair cell rows. Scale bars: 6 μm.

are interpreted within hair cells by a cell-intrinsic effector machinery. These cell-intrinsic processes are capable of operating independently of inputs from the tissue polarity pathway to drive planar polarization of individual cells, as core PCP genes are not required for establishing planar polarity features including polarized basal body position, V-shaped hair bundle and the asymmetric cortical domain of Rac-PAK activity.

We show that the asymmetric localization of Dvl2 is maintained when *Lis1* is deleted predominantly in hair cells, suggesting that tissue polarity cues set up by the core PCP pathway remain intact. We propose that Lis1 is a component of the cell-intrinsic effector machinery in embryonic hair cells that controls localized cortical Rac-PAK activity through microtubule-mediated transport. At the onset of planar polarization, the arrival of the basal body at the lateral pole of the hair cell tightly correlates with asymmetric cortical PAK activity (Grimsley-Myers et al., 2009). Importantly, hair cell planar polarization is disrupted in *Kif3a*-deficient hair cells, where active PAK on the cell cortex is mislocalized and diffuse, indicating that plus-end-directed transport is important for constraining the cortical domain of Rac-PAK signaling (Sipe and Lu, 2011). Here we show a correlation between reduced cortical Rac-PAK signaling and microtubule organization defects in *Lis1*$^{cKO\text{-}early}$ hair cells, suggesting that Lis1-dependent microtubule organization is crucial for Rac-PAK activation on the cell cortex. Lis1 also appears to regulate Rac activity in the pericentriolar region, which is likely to control hair bundle cohesion and the position of the kinocilium within the hair bundle. Furthermore, we show that the Rac GEF Tiam1 is associated with microtubules in a manner that is sensitive to microtubule organization and developmentally regulated, making Tiam1 a strong candidate activator of cortical Rac-PAK signaling during the planar polarization of hair cells.

Taken together, these results suggest a model whereby microtubule-associated Tiam1 translocates to the cell cortex through Lis1-mediated microtubule-cell cortex interactions to stimulate cortical Rac-PAK activation (Fig. 9A). Migration of the basal body to the hair cell periphery is the symmetry-breaking event that sets the cell-intrinsic effector machinery in motion. Following migration of the basal body to the hair cell periphery, centriolar microtubules interact with the nearby cell cortex, allowing translocation of Tiam1 from microtubules to the cell cortex, which enables it to activate Rac-PAK signaling (Michiels et al., 1997). This cortical Rac-PAK activity strengthens local interactions between microtubules and the cell cortex through as yet unidentified cortical and cytoskeletal proteins, thus setting up a positive-feedback loop that establishes the constrained domain of Rac-PAK signaling essential for proper positioning of the basal body (Fig. 9A). Lis1 could regulate microtubule-cell cortex interactions directly by binding to cortical proteins, such as Iqgap1 (Kholmanskikh et al., 2006), and/or indirectly through dynein-mediated cortical capture of microtubules (Laan et al., 2012; Markus et al., 2009; Tsai et al., 2005; Yamada et al., 2008). Of note, similar mechanisms involving feedback loops between Rho family GTPases and polarized trafficking via the cytoskeleton have been proposed for self-polarization of unicellular organisms and other polarized cell types in the absence of extrinsic cues (Chang and Martin, 2009; Slaughter et al., 2009; Tahirovic and Bradke, 2009).

Acting upstream of the cell-intrinsic effector pathway, tissue-level PCP signaling may spatially coordinate cortical Rac-PAK activity through two potential mechanisms, which are not mutually exclusive. First, mechanical tension between hair cells and supporting cells may be involved in tissue-level PCP signaling. Genetic evidence suggests that the core PCP pathway acts in conjunction with a *Ptk7*-mediated pathway to modulate apical junctional actomyosin contractility (Lee et al., 2012; Lu et al., 2004). Anisotropic mechanical forces exerted on hair cells might bias the positioning of the basal body toward the lateral pole to

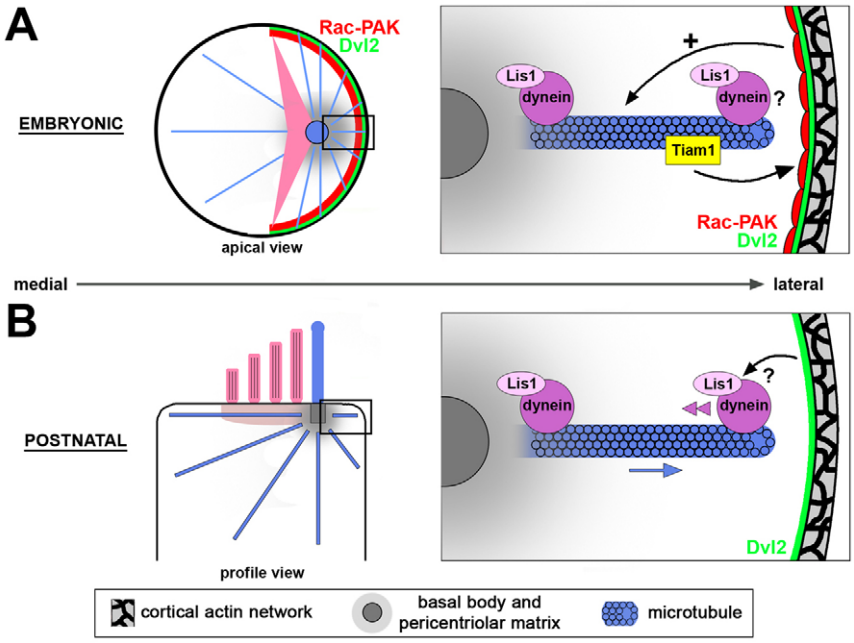

Fig. 9. Model for Lis1 function in hair cell planar polarity. (**A**) During mouse embryonic development, Lis1 regulates the organization of centriolar microtubules and their interactions with the nearby cell cortex. These interactions allow cortical translocation of microtubule-associated Tiam1, leading to local activation of Rac-PAK signaling. In turn, localized Rac-PAK activity serves as a polarity cue to position the basal body. The core PCP pathway spatially orients the cortical domain of Rac-PAK signaling. (**B**) In postnatal hair cells, Lis1 regulates both pericentriolar matrix organization and cortical dynein, which together allow generation of the pulling force on centriolar microtubules that is necessary to maintain centrosome positioning. The core PCP pathway may coordinate with cortical proteins to spatially regulate dynein activity.

orient centriolar microtubules and align planar polarity in embryonic hair cells. In addition to actomyosin-mediated forces, the core PCP pathway may also regulate dynein-mediated microtubule capture at the hair cell cortex. Interestingly, dishevelled has been shown to regulate dynein-mediated mitotic spindle orientation through interaction with nuclear mitotic apparatus protein (NuMA) in other systems (Ségalen et al., 2010). NuMA, together with LGN (leucine-glycine-asparagine repeat-enriched protein) and Gα, forms an evolutionarily conserved cortical protein complex that recruits cytoplasmic dynein to the cell cortex to generate pulling forces that position spindle microtubules (Johnston et al., 2009; Nguyen-Ngoc et al., 2007). Recently, G protein-signaling modulator 2 (*GPSM2*), the human homolog of *LGN*, has been identified as the causative gene for the nonsyndromic deafness DFNB82 (Walsh et al., 2010; Yariz et al., 2012). Thus, we speculate that a dishevelled-dynein pathway analogous to that which mediates mitotic spindle orientation might regulate cortical microtubule capture, thereby orienting centriolar microtubules in both embryonic and postnatal hair cells (Fig. 9).

In postnatal *Lis1*$^{cKO\text{-}late}$ hair cells, planar polarity is established normally but is subsequently lost, as indicated by the observed basal body anchoring and bundle morphology defects. This is, to our knowledge, the first direct evidence that hair cell planar polarity must be actively maintained during early postnatal development. In contrast to embryonic hair cells, cortical Rac activity is significantly downregulated in P3 hair cells, suggesting that asymmetric cortical Rac-PAK activity is crucial for the initial planar polarization process but that alternative mechanisms are employed to maintain planar polarity. Our data suggest that dishevelled might act upstream of Lis1-dynein to maintain the centrosome position in postnatal hair cells.

Intriguingly, microtubule arrays were often more tightly focused around the centrosome in *Lis1*$^{cKO\text{-}late}$ hair cells, consistent with loss of cortical anchoring of microtubule plus ends. In other systems, cortical dynein plays an essential role in the regulation of microtubule growth and exerts pulling forces to position microtubule associated-structures (Etienne-Manneville and Hall, 2001; Gundersen and Bulinski, 1988; Laan et al., 2012; Palazzo et al., 2001; Vallee and Stehman, 2005). The buckling and bending of long microtubules around the cell cortex observed in a subset of *Lis1*$^{cKO\text{-}late}$ hair cells is similar to the *in vitro* behavior of microtubules in the absence of end-on capture by cortical dynein (Laan et al., 2012). Based on these observations, we propose that Lis1-dynein-mediated cortical capture of microtubules, together with a microtubule-organizing function at the centrosome, controls anchoring of the basal body at the lateral pole of hair cells. Proper basal body position, in turn, maintains the V-shape of the hair bundle during early postnatal development (Fig. 9B).

Although defects in dynein and microtubule organization were widespread in *Lis1*$^{cKO\text{-}late}$ hair cells, only a subset develops flat or split hair bundles, suggesting that hair cells employ redundant mechanisms for maintaining proper hair bundle morphology. During early postnatal development, the apical region of the hair cell undergoes a shape change driven by actomyosin forces (Etournay et al., 2010). Also during this time period, densely bundled rootlet structures form at the base of the stereocilia to anchor them into the cuticular plate, an actin meshwork that provides rigid support (DeRosier and Tilney, 1989; Kitajiri et al., 2010). We suggest that the rootlets of the stereocilia and the cuticular plate serve as additional physical constraints to maintain the position of the basal body and the V-shape of the hair bundle in conjunction with Lis1-dynein. Lis1 is also required for positioning of the Golgi and mitochondria, as well as for hair cell survival. Importantly, cell death is not limited to cells with abnormal hair bundles, suggesting that it is not merely a consequence of hair bundle defects. Further study is needed to understand these additional functions of Lis1-dynein.

Acknowledgements
We thank Drs Lin Gan (University of Rochester Medical Center), Andreas Merdes and Kevin Pfister for reagents.

Funding
This study was supported by the National Institutes of Health (NIH) [grant R01 DC009238 to X.L.; NIH training grant T32 GM008136 to C.W.S. for Cell and Molecular Biology at the University of Virginia]. Deposited in PMC for release after 12 months.

Competing interests statement
The authors declare no competing financial interests.

Supplementary material
Supplementary material available online at
http://dev.biologists.org/lookup/suppl/doi:10.1242/dev.089763/-/DC1

References

Akbar, H., Cancelas, J., Williams, D. A., Zheng, J. and Zheng, Y. (2006). Rational design and applications of a Rac GTPase-specific small molecule inhibitor. *Methods Enzymol.* **406**, 554-565.

Balczon, R., Bao, L. and Zimmer, W. E. (1994). PCM-1, A 228-kD centrosome autoantigen with a distinct cell cycle distribution. *J. Cell Biol.* **124**, 783-793.

Chang, F. and Martin, S. G. (2009). Shaping fission yeast with microtubules. *Cold Spring Harb. Perspect. Biol.* **1**, a001347.

Dabdoub, A., Donohue, M. J., Brennan, A., Wolf, V., Montcouquiol, M., Sassoon, D. A., Hseih, J.-C., Rubin, J. S., Salinas, P. C. and Kelley, M. W. (2003). Wnt signaling mediates reorientation of outer hair cell stereociliary bundles in the mammalian cochlea. *Development* **130**, 2375-2384.

Dammermann, A. and Merdes, A. (2002). Assembly of centrosomal proteins and microtubule organization depends on PCM-1. *J. Cell Biol.* **159**, 255-266.

Denman-Johnson, K. and Forge, A. (1999). Establishment of hair bundle polarity and orientation in the developing vestibular system of the mouse. *J. Neurocytol.* **28**, 821-835.

DeRosier, D. J. and Tilney, L. G. (1989). The structure of the cuticular plate, an in vivo actin gel. *J. Cell Biol.* **109**, 2853-2867.

Dillman, J. F., III and Pfister, K. K. (1994). Differential phosphorylation in vivo of cytoplasmic dynein associated with anterogradely moving organelles. *J. Cell Biol.* **127**, 1671-1681.

Etienne-Manneville, S. and Hall, A. (2001). Integrin-mediated activation of Cdc42 controls cell polarity in migrating astrocytes through PKCzeta. *Cell* **106**, 489-498.

Etournay, R., Lepelletier, L., Boutet de Monvel, J., Michel, V., Cayet, N., Leibovici, M., Weil, D., Foucher, I., Hardelin, J.-P. and Petit, C. (2010). Cochlear outer hair cells undergo an apical circumference remodeling constrained by the hair bundle shape. *Development* **137**, 1373-1383.

Gambello, M. J., Darling, D. L., Yingling, J., Tanaka, T., Gleeson, J. G. and Wynshaw-Boris, A. (2003). Multiple dose-dependent effects of Lis1 on cerebral cortical development. *J. Neurosci.* **23**, 1719-1729.

Goodrich, L. V. and Strutt, D. (2011). Principles of planar polarity in animal development. *Development* **138**, 1877-1892.

Grimsley-Myers, C. M., Sipe, C. W., Géléoc, G. S. G. and Lu, X. (2009). The small GTPase Rac1 regulates auditory hair cell morphogenesis. *J. Neurosci.* **29**, 15859-15869.

Gundersen, G. G. and Bulinski, J. C. (1988). Selective stabilization of microtubules oriented toward the direction of cell migration. *Proc. Natl. Acad. Sci. USA* **85**, 5946-5950.

Guo, J., Yang, Z., Song, W., Chen, Q., Wang, F., Zhang, Q. and Zhu, X. (2006). Nudel contributes to microtubule anchoring at the mother centriole and is involved in both dynein-dependent and -independent centrosomal protein assembly. *Mol. Biol. Cell* **17**, 680-689.

Harada, A, Takei, Y., Kanai, Y., Tanaka, Y., Nonaka, S. and Hirokawa, N. (1998). Golgi vesiculation and lysosome dispersion in cells lacking cytoplasmic dynein. *J. Cell Biol.* **141**, 51-59.

Higginbotham, H., Bielas, S., Tanaka, T. and Gleeson, J. G. (2004). Transgenic mouse line with green-fluorescent protein-labeled Centrin 2 allows visualization of the centrosome in living cells. *Transgenic Res.* **13**, 155-164.

Hirotsune, S., Fleck, M. W., Gambello, M. J., Bix, G. J., Chen, A., Clark, G. D., Ledbetter, D. H., McBain, C. J. and Wynshaw-Boris, A. (1998). Graded reduction of Pafah1b1 (Lis1) activity results in neuronal migration defects and early embryonic lethality. *Nat. Genet.* **19**, 333-339.

Huang, J., Roberts, A. J., Leschziner, A. E. and Reck-Peterson, S. L. (2012). Lis1 acts as a "clutch" between the ATPase and microtubule-binding domains of the dynein motor. *Cell* **150**, 975-986.

Johnston, C. A., Hirono, K., Prehoda, K. E. and Doe, C. Q. (2009). Identification of an Aurora-A/PinsLINKER/Dlg spindle orientation pathway using induced cell polarity in S2 cells. *Cell* **138**, 1150-1163.

Jones, C., Roper, V. C., Foucher, I., Qian, D., Banizs, B., Petit, C., Yoder, B. K. and Chen, P. (2008). Ciliary proteins link basal body polarization to planar cell polarity regulation. *Nat. Genet.* **40**, 69-77.

Kazmierczak, P. and Müller, U. (2012). Sensing sound: molecules that orchestrate mechanotransduction by hair cells. *Trends Neurosci.* **35**, 220-229.

Kholmanskikh, S. S., Dobrin, J. S., Wynshaw-Boris, A., Letourneau, P. C. and Ross, M. E. (2003). Disregulated RhoGTPases and actin cytoskeleton contribute to the migration defect in Lis1-deficient neurons. *J. Neurosci.* **23**, 8673-8681.

Kholmanskikh, S. S., Koeller, H. B., Wynshaw-Boris, A., Gomez, T., Letourneau, P. C. and Ross, M. E. (2006). Calcium-dependent interaction of Lis1 with IQGAP1 and Cdc42 promotes neuronal motility. *Nat. Neurosci.* **9**, 50-57.

Kitajiri, S., Sakamoto, T., Belyantseva, I. A., Goodyear, R. J., Stepanyan, R., Fujiwara, I., Bird, J. E., Riazuddin, S., Riazuddin, S., Ahmed, Z. M. et al. (2010). Actin-bundling protein TRIOBP forms resilient rootlets of hair cell stereocilia essential for hearing. *Cell* **141**, 786-798.

Kubo, A., Sasaki, H., Yuba-Kubo, A., Tsukita, S. and Shiina, N. (1999). Centriolar satellites: molecular characterization, ATP-dependent movement toward centrioles and possible involvement in ciliogenesis. *J. Cell Biol.* **147**, 969-980.

Kunda, P., Paglini, G., Quiroga, S., Kosik, K. and Caceres, a (2001). Evidence for the involvement of Tiam1 in axon formation. *J. Neurosci.* **21**, 2361-2372.

Laan, L., Pavin, N., Husson, J., Romet-Lemonne, G., van Duijn, M., López, M. P., Vale, R. D., Jülicher, F., Reck-Peterson, S. L. and Dogterom, M. (2012). Cortical dynein controls microtubule dynamics to generate pulling forces that position microtubule asters. *Cell* **148**, 502-514.

Lam, C., Vergnolle, M. A., Thorpe, L., Woodman, P. G. and Allan, V. J. (2010). Functional interplay between LIS1, NDE1 and NDEL1 in dynein-dependent organelle positioning. *J. Cell Sci.* **123**, 202-212.

Lee, J., Andreeva, A., Sipe, C. W., Liu, L., Cheng, A. and Lu, X. (2012). PTK7 regulates myosin II activity to orient planar polarity in the mammalian auditory epithelium. *Curr. Biol.* **22**, 956-966.

Lu, X., Borchers, A. G. M., Jolicoeur, C., Rayburn, H., Baker, J. C. and Tessier-Lavigne, M. (2004). PTK7/CCK-4 is a novel regulator of planar cell polarity in vertebrates. *Nature* **430**, 93-98.

Markus, S. M., Punch, J. J. and Lee, W.-L. (2009). Motor- and tail-dependent targeting of dynein to microtubule plus ends and the cell cortex. *Curr. Biol.* **19**, 196-205.

McKenney, R. J., Vershinin, M., Kunwar, A., Vallee, R. B. and Gross, S. P. (2010). LIS1 and NudE induce a persistent dynein force-producing state. *Cell* **141**, 304-314.

Michiels, F., Stam, J. C., Hordijk, P. L., van der Kammen, R. A., Ruuls-Van Stalle, L., Feltkamp, C. A. and Collard, J. G. (1997). Regulated membrane localization of Tiam1, mediated by the NH2-terminal pleckstrin homology domain, is required for Rac-dependent membrane ruffling and C-Jun NH2-terminal kinase activation. *J. Cell Biol.* **137**, 387-398.

Nguyen-Ngoc, T., Afshar, K. and Gönczy, P. (2007). Coupling of cortical dynein and G alpha proteins mediates spindle positioning in Caenorhabditis elegans. *Nat. Cell Biol.* **9**, 1294-1302.

Palazzo, A. F., Joseph, H. L., Chen, Y. J., Dujardin, D. L., Alberts, A. S., Pfister, K. K., Vallee, R. B. and Gundersen, G. G. (2001). Cdc42, dynein, and dynactin regulate MTOC reorientation independent of Rho-regulated microtubule stabilization. *Curr. Biol.* **11**, 1536-1541.

Quintyne, N. J., Gill, S. R., Eckley, D. M., Crego, C. L., Compton, D. A. and Schroer, T. A. (1999). Dynactin is required for microtubule anchoring at centrosomes. *J. Cell Biol.* **147**, 321-334.

Rehberg, M., Kleylein-Sohn, J., Faix, J., Ho, T. H., Schulz, I. and Gräf, R. (2005). Dictyostelium LIS1 is a centrosomal protein required for microtubule/cell cortex interactions, nucleus/centrosome linkage, and actin dynamics. *Mol. Biol. Cell* **16**, 2759-2771.

Rooney, C., White, G., Nazgiewicz, A., Woodcock, S. A., Anderson, K. I., Ballestrem, C. and Malliri, A. (2010). The Rac activator STEF (Tiam2) regulates cell migration by microtubule-mediated focal adhesion disassembly. *EMBO Rep.* **11**, 292-298.

Sasaki, S., Shionoya, A., Ishida, M., Gambello, M. J., Yingling, J., Wynshaw-Boris, A. and Hirotsune, S. (2000). A LIS1/NUDEL/cytoplasmic dynein heavy chain complex in the developing and adult nervous system. *Neuron* **28**, 681-696.

Ségalen, M., Johnston, C. A., Martin, C. A., Dumortier, J. G., Prehoda, K. E., David, N. B., Doe, C. Q. and Bellaïche, Y. (2010). The Fz-Dsh planar cell polarity pathway induces oriented cell division via Mud/NuMA in Drosophila and zebrafish. *Dev. Cell* **19**, 740-752.

Sipe, C. W. and Lu, X. (2011). Kif3a regulates planar polarization of auditory hair cells through both ciliary and non-ciliary mechanisms. *Development* **138**, 3441-3449.

Slaughter, B. D., Smith, S. E. and Li, R. (2009). Symmetry breaking in the life cycle of the budding yeast. *Cold Spring Harb. Perspect. Biol.* **1**, a003384.

Smith, D. S., Niethammer, M., Ayala, R., Zhou, Y., Gambello, M. J., Wynshaw-Boris, A. and Tsai, L. H. (2000). Regulation of cytoplasmic dynein behaviour and microtubule organization by mammalian Lis1. *Nat. Cell Biol.* **2**, 767-775.

Steyger, P. S., Furness, D. N., Hackney, C. M. and Richardson, G. P. (1989). Tubulin and microtubules in cochlear hair cells: comparative immunocytochemistry and ultrastructure. *Hear. Res.* **42**, 1-16.

Tahirovic, S. and Bradke, F. (2009). Neuronal polarity. *Cold Spring Harb. Perspect. Biol.* **1**, a001644.

Tanaka, T., Serneo, F. F., Higgins, C., Gambello, M. J., Wynshaw-Boris, A. and Gleeson, J. G. (2004). Lis1 and doublecortin function with dynein to mediate coupling of the nucleus to the centrosome in neuronal migration. *J. Cell Biol.* **165**, 709-721.

Tilney, L. G., Tilney, M. S. and DeRosier, D. J. (1992). Actin filaments, stereocilia, and hair cells: how cells count and measure. *Annu. Rev. Cell Biol.* **8**, 257-274.
Togashi, H., Kominami, K., Waseda, M., Komura, H., Miyoshi, J., Takeichi, M. and Takai, Y. (2011). Nectins establish a checkerboard-like cellular pattern in the auditory epithelium. *Science* **333**, 1144-1147.
Tsai, J.-W., Chen, Y., Kriegstein, A. R. and Vallee, R. B. (2005). LIS1 RNA interference blocks neural stem cell division, morphogenesis, and motility at multiple stages. *J. Cell Biol.* **170**, 935-945.
Vallee, R. B. and Stehman, S. A. (2005). How dynein helps the cell find its center: a servomechanical model. *Trends Cell Biol.* **15**, 288-294.
Vallee, R. B. and Tsai, J.-W. (2006). The cellular roles of the lissencephaly gene LIS1, and what they tell us about brain development. *Genes Dev.* **20**, 1384-1393.
Vallee, R. B., McKenney, R. J. and Ori-McKenney, K. M. (2012). Multiple modes of cytoplasmic dynein regulation. *Nat. Cell Biol.* **14**, 224-230.
Walsh, T., Shahin, H., Elkan-Miller, T., Lee, M. K., Thornton, A. M., Roeb, W., Abu Rayyan, A., Loulus, S., Avraham, K. B., King, M.-C. et al. (2010). Whole exome sequencing and homozygosity mapping identify mutation in the cell polarity protein GPSM2 as the cause of nonsyndromic hearing loss DFNB82. *Am. J. Hum. Genet.* **87**, 90-94.
Webb, S. W., Grillet, N., Andrade, L. R., Xiong, W., Swarthout, L., Della Santina, C. C., Kachar, B. and Müller, U. (2011). Regulation of PCDH15 function in mechanosensory hair cells by alternative splicing of the cytoplasmic domain. *Development* **138**, 1607-1617.
Wynshaw-Boris, A., Pramparo, T., Youn, Y. H. and Hirotsune, S. (2010). Lissencephaly: mechanistic insights from animal models and potential therapeutic strategies. *Semin. Cell Dev. Biol.* **21**, 823-830.
Yamada, M., Toba, S., Yoshida, Y., Haratani, K., Mori, D., Yano, Y., Mimori-Kiyosue, Y., Nakamura, T., Itoh, K., Fushiki, S. et al. (2008). LIS1 and NDEL1 coordinate the plus-end-directed transport of cytoplasmic dynein. *EMBO J.* **27**, 2471-2483.
Yang, H., Xie, X., Deng, M., Chen, X. and Gan, L. (2010). Generation and characterization of Atoh1-Cre knock-in mouse line. *Genesis* **48**, 407-413.
Yariz, K. O., Walsh, T., Akay, H., Duman, D., Akkaynak, A. C., King, M. C. and Tekin, M. (2012). A truncating mutation in GPSM2 is associated with recessive non-syndromic hearing loss. *Clin. Genet.* **81**, 289-293.
Zimmerman, W. and Doxsey, S. J. (2000). Construction of centrosomes and spindle poles by molecular motor-driven assembly of protein particles. *Traffic* **1**, 927-934.

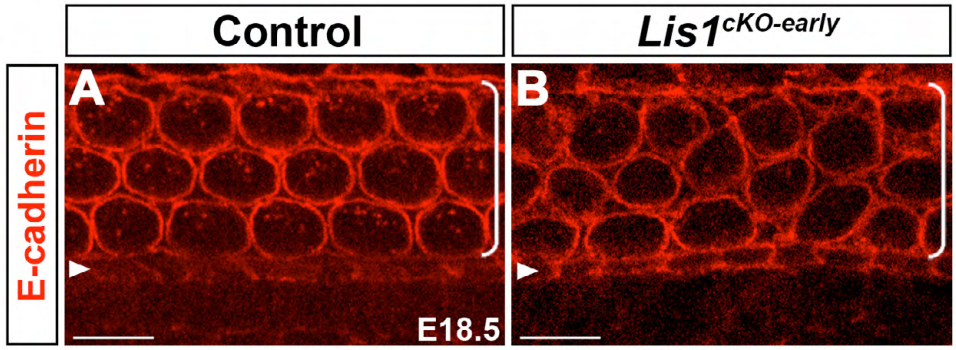

Fig. S1. Normal junctional E-cadherin localization in *Lis1*$^{cKO\text{-}early}$ hair cells. E-cadherin immunostaining (red) in E18.5 control (**A**) and *Lis1*$^{cKO\text{-}early}$ (**B**) organ of Corti at the level of the adherens junctions. Arrowheads mark the pillar cell row and brackets indicate outer hair cell rows. Scale bars: 6 μm.

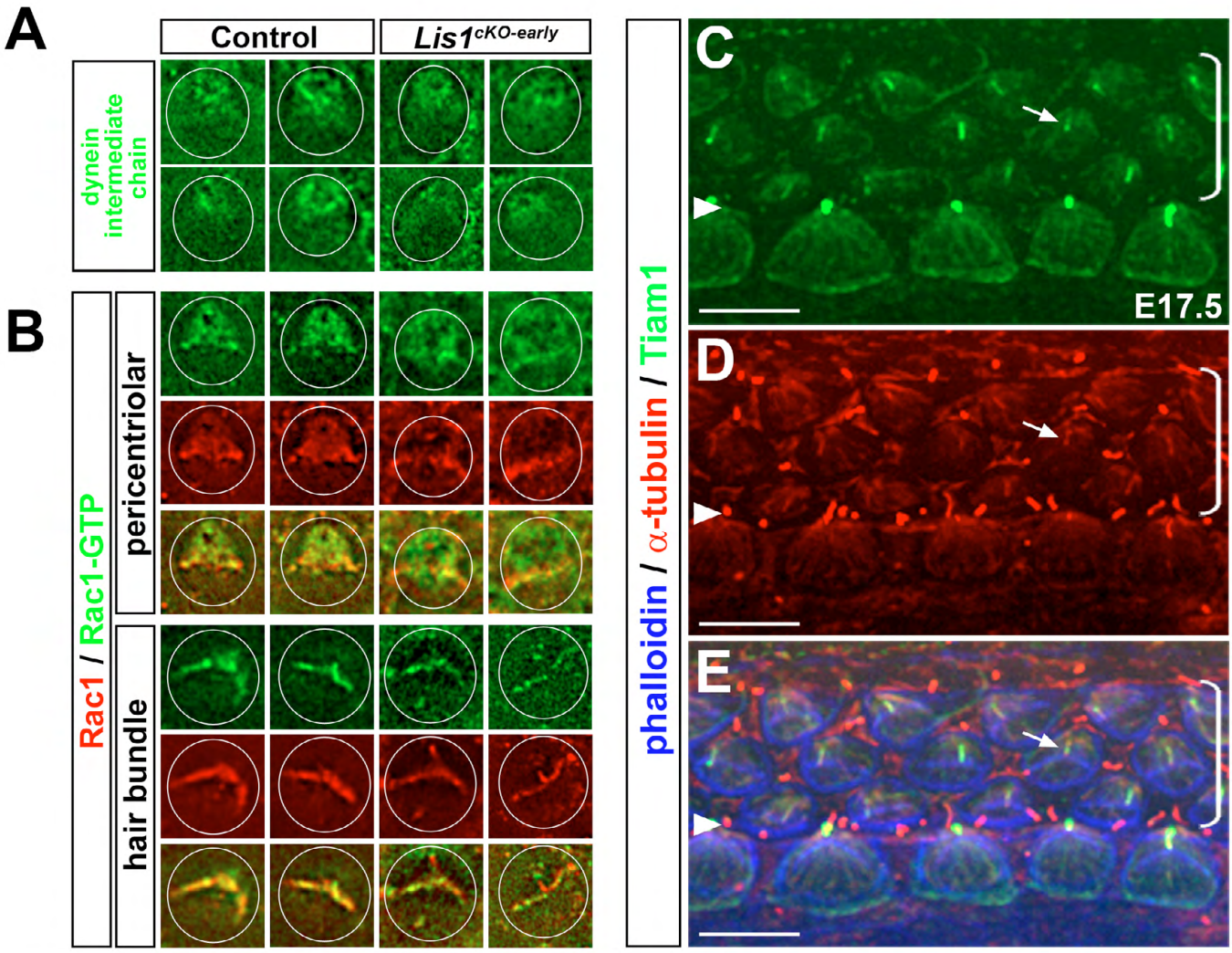

Fig. S2. Subcellular localization of dynein, Rac1-GTP and Tiam1 in hair cells at E17.5. (**A**) Dynein intermediate chain immunostaining (green) in individual control (left) and *Lis1*$^{cKO\text{-}early}$ (right) hair cells. Dynein in control hair cells is enriched in the pericentriolar region. In *Lis1*$^{cKO\text{-}early}$ hair cells, dynein staining in the pericentriolar region is more diffuse. (**B**) Rac1-GTP (green) and Rac1 (red) immunostaining in individual control (left) and *Lis1*$^{cKO\text{-}early}$ (right) hair cells. Each panel is an optical section taken at the level of the hair cell centrosome or the hair bundle as indicated. White circles mark individual hair cell boundaries. (**C-E**) Tiam1 (green) and α-tubulin (red) immunostaining in a wild-type organ of Corti. Tiam1 is enriched on the hair cell kinocilium (arrows). Arrowheads mark the pillar cell row and brackets indicate outer hair cell rows. Scale bars: 6 μm.

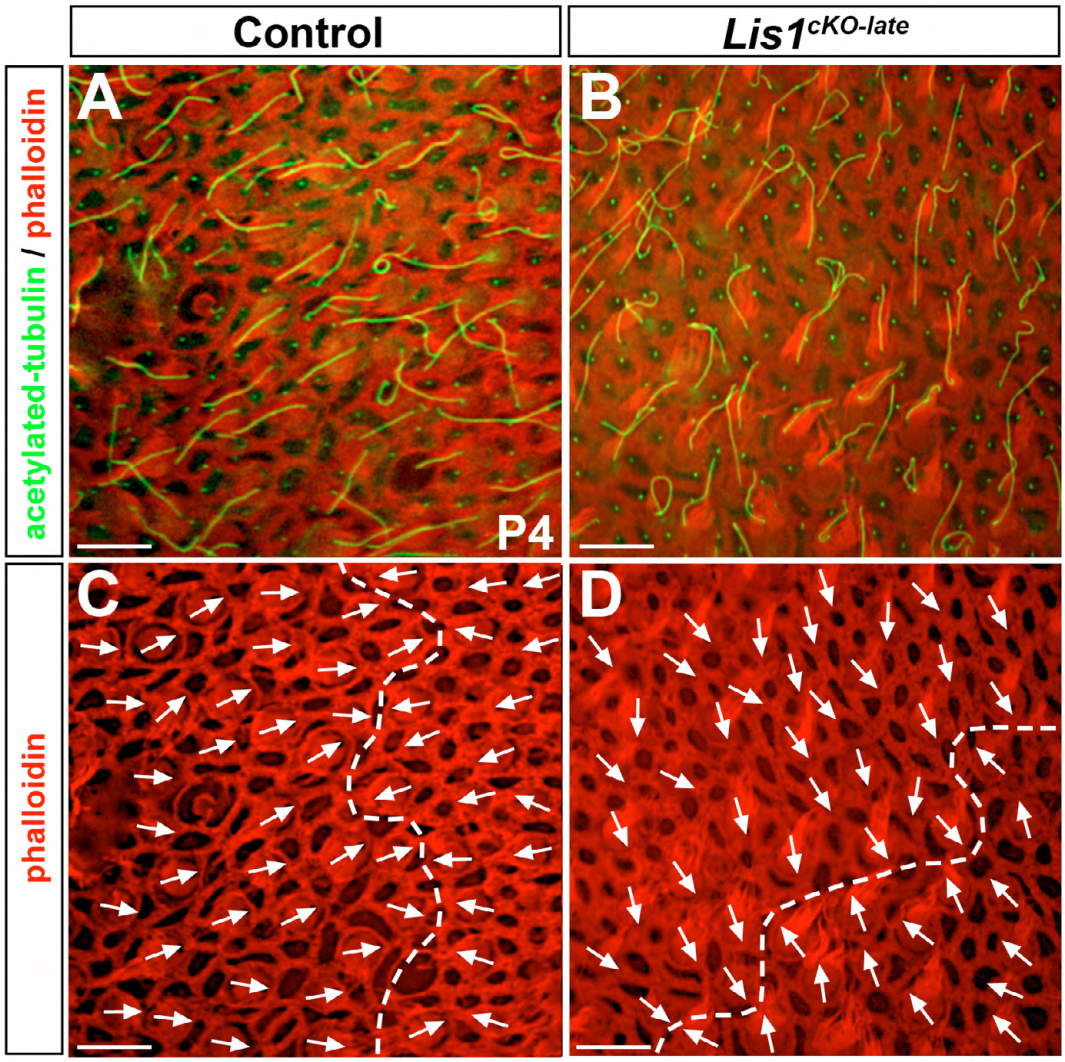

Fig. S3. Normal hair bundle morphology and polarity in the *Lis1*$^{cKO\text{-}late}$ utricle. Acetylated-tubulin (green) and phalloidin (red) staining in P4 control (A,C) and *Lis1*$^{cKO\text{-}late}$ (B,D) utricles. (**A**,**B**) Hair bundle morphology and kinocilium position are normal in *Lis1*$^{cKO\text{-}late}$ utricular hair cells (B) compared with controls (A). (**C**,**D**) Planar polarity of hair cells appears normal in *Lis1*$^{cKO\text{-}late}$ utricles (D) compared with controls (C). Panels show *z*-sections taken at the level of the cuticular plate. Arrows indicate planar polarity as revealed by actin staining of the cuticular plate. Dashed lines indicate the line of reversal. Scale bars: 6 μm.

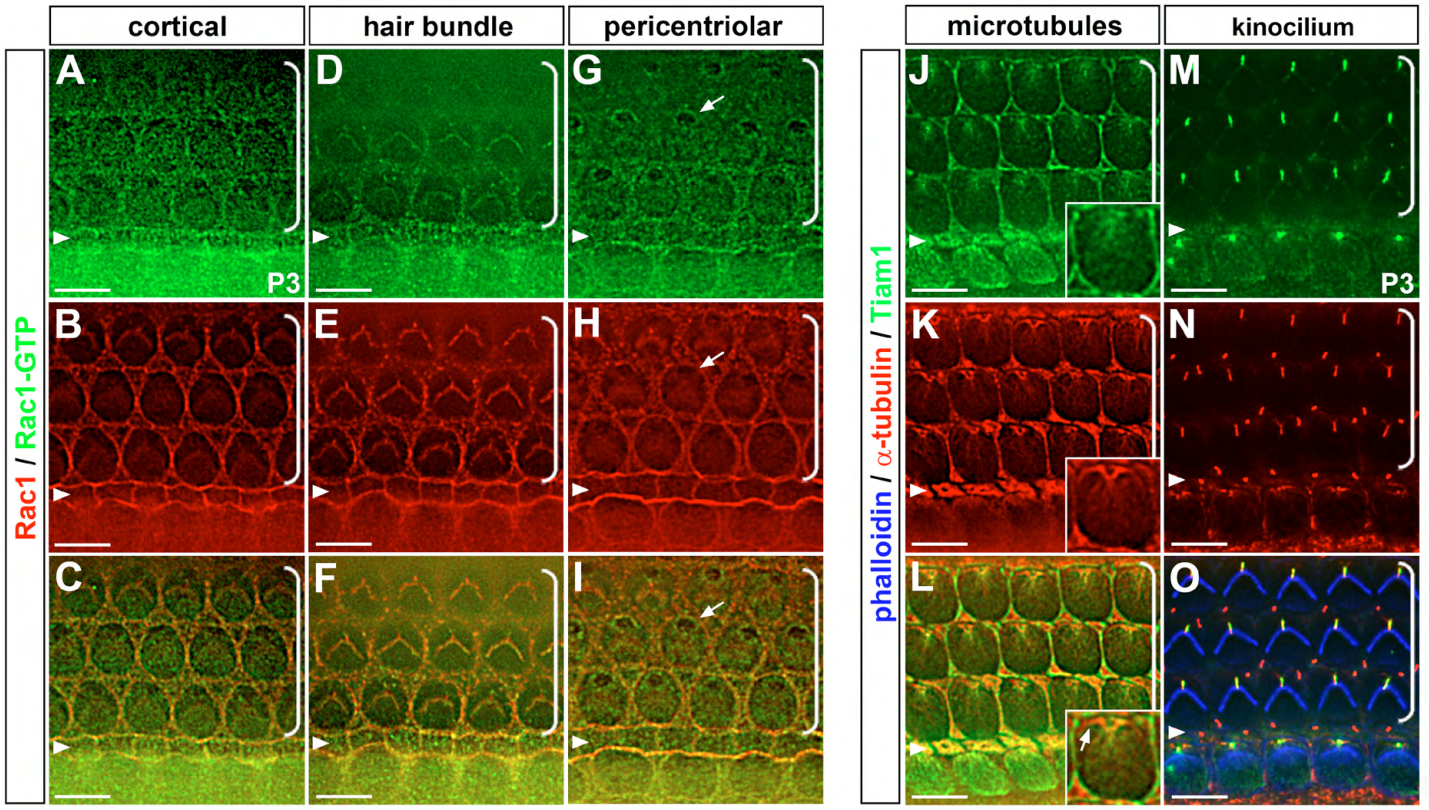

Fig. S4. Rac1-GTP and Tiam1 localization in wild-type organ of Corti at P3. (**A-I**) Rac1-GTP (green) and total Rac1 (red) immunostaining at the level of Dvl2 cortical crescents (A-C), the hair bundle (D-F) and the pericentriolar region (G-I). (**J-O**) Tiam1 (green) and α-tubulin (red) immunostaining at the level of centriolar microtubules (J-L) and the kinocilium (M-O). Tiam1 localization on microtubules is restricted to the pericentriolar region (J-L); bundled microtubules along the cell cortex lack significant Tiam1 staining (insets, arrow). Arrowheads mark the pillar cell row and brackets indicate outer hair cell rows. Scale bars: 6 μm.